Supporting Information

Efficient Non-Doped Blue Electroluminescence Based on Phenanthroimidazole–Benzoylfluorene Hybrid Molecules with High Spin-Orbit Coupling and Balanced Charge Mobilities

Yannan Zhou,[a] Mingliang Xie,[a] Xin Wang,[a] Mizhen Sun,[a] Huayi Zhou,[a] Shi-Tong Zhang,[b]* Wenjun Yang [a] and Shanfeng Xue,[a]*

[a] Key Laboratory of Rubber-Plastics of the Ministry of Education, School of Polymer Science & Engineering, Qingdao University of Science and Technology, 53-Zhengzhou Road, Qingdao 266042, P. R. China.

*Corresponding author. E-mail: sfxue@qust.edu.cn;

[b] State Key Laboratory of Supramolecular Structure and Materials, Institute of Theoretical Chemistry, College of Chemistry, Jilin University, Changchun 130012, P. R. China.

E-mail: stzhang@jlu.edu.cn

Table of Contents

S1 Materials and Measurements

General Measurements: ^{1}H and ^{13}C NMR spectra were recorded on a Bruker AC-500 spectrometer at 400/500 MHz and 125 MHz, respectively, when the compounds were dissolved in deuterated chloroform-d ($CDCl_3$) with 0.03% tetramethylsilane (TMS) as the internal standard. The high resolution mass spectra were measured using an Agilent 7890B-7000C instrument. UV-vis absorption and fluorescence spectra of solution and films were measured by the Hitachi U-4100 spectrophotometer and Hitachi F-4600 spectrophotometer, respectively. Photoluminescence quantum yield was carried out with HAMAMATSU Quantaurus-QY. The lifetimes of non-doped films were measured on an Edinburgh FLS-1000 with an EPL-375 optical laser.

Thermal Stability Measurements: Differential scanning calorimetry (DSC) curves were determined on a Netzsch DSC (204F1) instrument at a heating rate of 10 °C min^{-1}. Thermogravimetric analysis (TGA) was performed on a Netzsch (209F1) thermogravimetric analyzer in a nitrogen atmosphere (50 mL min^{-1}) at a heating rate of 10 °C min^{-1}.

Electrochemical Measurements: Cyclic voltammetry (CV) was performed with a CH CHI600 series electrochemical workstation using a glass carbon disk (diameter = 3 mm) as the working electrode, a platinum wire with a porous ceramic wick as the auxiliary electrode, and Ag/Ag^+ as the reference electrode standardized by the redox couple ferrocenium/ferrocene. All solutions were purged with a nitrogen stream for 10 min before measurement. The procedure was performed at room temperature. Oxidation

tests were performed in CH_2Cl_2 and reduction tests were in DMF. The calculation of HOMO and LUMO is based on the Eq. (S1).

$$HOMO = - [(E_{ox} - F_{1/2}^+) + 4.8] \text{ eV}$$

$$LUMO = - [(E_{red} - F_{1/2}^-) + 4.8] \text{ eV} \tag{S1}$$

Where E_{ox} and E_{red} represents oxidation and reduction potentials, $F_{1/2}^+$ and $F_{1/2}^-$ represents half wave potentials of ferrocene obtained from positive and negative CV scans, respectively.

Materials: All raw materials involved in the synthesis process were purchased from Aldrich Chemical Co. or Energy Chemical Co., China. The organic and metallic materials for transporting layers in OLEDs fabrication were purchased from P-OLED(Shanghai) Technology CO., LTO. Tetrahydrofuran (THF) was distilled over metallic sodium before use. The other organic solvents and reagents were all commercially available analytical-grade products and were used as received without further purification. Vacuum sublimation of the final product was carried out to further improve the purity before investigating the photoluminescence (PL) and electroluminescence (EL) properties.

Theoretical calculation: The ground-state geometry was optimized at the level of B3LYP/6-31g(d,p), spatial distributions of the HOMOs and LUMOs of the compound was obtained from the optimized ground state structure. On the basis of the optimized configuration of the ground state (S_0), the high excitation energy levels of singlet and triplet states were evaluated using wB97XD/6-31G (d, p) (w=01391). In order to gain further insight into the character of excited states, natural transition orbitals (NTOs) were evaluated for $S_1 - S_{10}$ and $T_1 - T_{10}$ states. The SOC values were calculated based

on the optimal geometry of T1 state by using ORCA software package Version 5.0.3 at M062X/def2-SVP level.

Device fabrication.: ITO-coated glass with a sheet resistance of 15–20 Ω cm^{-2} was used as the substrate. Before device fabrication, the ITO glass substrates were cleaned with ethanol, acetone, ITO washing solution, then dried in an oven at 120 °C. After oxygen plasma cleaning for 6 min and finally transferred to a vacuum deposition system with a base pressure greater than 2×10^{-4} Pa for organic and metal deposition. The thickness of each deposition layer was monitored using a quartz crystal thickness/ratio monitor. The current-voltage-luminance characteristics were measured by using a Keuthley source measurement unit (Keuthley 2450 sourcemeter and LS-160 luminance meter). The EL spectra and EQEs were measured by Ocean Insight flame miniature spectrometer.

Carrier mobility measurement: The SCLC method can be described via the Mott-Gurney Eq. (S2), and the carrier mobility (μ) of organic semiconductors can be calculated according to the Poole–Frenkel Eq. (S2), where the ε_0 is the free-space permittivity (8.85×10^{-14} C V^{-1} cm^{-1}), ε_r is the relative dielectric constant (assumed to be 3.0 for organic semiconductors), E is the electric field, μ_0 is the zero-field mobility, and γ is the Poole-Frenkel factor and L is the thickness of the neat film of each molecule.

$$J = \frac{9}{8}\varepsilon_0\varepsilon_r\frac{V^2}{L^3}\mu_0 e^{0.891\gamma\sqrt{\frac{V}{L}}}$$

(S2)

$$\mu = \mu_0 e^{\gamma\sqrt{E}}$$

(S3)

By fitting the current density–voltage curves in SCLC region according to Eq. (S3), the μ_0 and γ values are obtained, thus generating field-dependent carrier mobility by Eq. (S3).[2]

The efficiency roll-off (η): The efficiency roll-offs of OLED were calculated from maximum EQE (EQE_{max}) and the EQE at luminescence of 1000 cd m^{-2} (EQE_{1000}). According to equation following (Formula R1):

$$\eta = \frac{EQE_{max} - EQE_{1000}}{EQE_{max}} \tag{S4}$$

The radiative transition rate (kr):

$$k_r = \frac{\phi_f}{\tau} \tag{S5}$$

Where ϕ_f is represent the fluorescence quantum efficiency and τ is represent the lifetime.

S2 Synthesis and Routines

(1) Synthesis of 2-(4-bromophenyl)-1-phenyl-1*H*-phenanthro [9,10-*d*] imidazole (M1)

The synthesis, processing steps and product confirmation of this reaction have been mentioned in another article from our group, see that article for details[1].

(2) 1-phenyl-2-(4-(4,4,5,5-tetramethyl-1,3,2-dioxaborolan-2-yl) phenyl)-1*H*-phena-nthro[9,10-*d*] imidazole (M2)

The synthesis, processing steps and product confirmation of this reaction have been mentioned in another article from our group, see that article for details.[1]

(3) Synthesis of (4-bromophenyl) (9*H*-fluoren-2-yl) methanone (M3)

A mixture of 9*H*-fluorene (2.00g, 12.03mmol), 4-bromobenzoyl chloride (2.64g, 12.03mmol) and Dichloromethane (50ml) were added in flask under nitrogen. Then adding $AlCl_3$(1.92g, 14.40mmol) into the bottle and the reaction mixture was left to react at room temperature overnight. The reaction mixture was extracted several times with dichloromethane and saturated saline. The extracted organic phase was used with anhydrous magnesium sulfate. After filtration and evaporation of the solvent, the residue was purified by silica gel column chromatography using dichloromethane/petroleum ether (1:1) as eluent. A white powder solid product was obtained (3.47 g, 82.6%).^{1}H NMR (500 MHz, Chloroform-d) δ 8.03 (s, 1H), 7.93 – 7.89 (m, 2H), 7.85 (dd, J = 7.9, 1.5 Hz, 1H), 7.76 – 7.72 (m, 2H), 7.71 – 7.67 (m, 2H), 7.64 (d, J = 7.3 Hz, 1H), 7.49 – 7.41 (m, 2H), 4.01 (s, 2H).

(4) Synthesis of (4-bromophenyl) (9,9-dipropyl-9*H*-fluoren-2-yl) methanone (M4)

A mixture of (4-bromophenyl) (9*H*-fluoren-2-yl) methanone (2.00g, 7.40mmol), potassium tert-butoxide (1.928g, 17.18mmol) and N, N-Dimethylformamide (50ml) were added in flask under nitrogen. The reaction system was heated to 60°C for 20 minutes. Then n-Propyl bromide (2.113g, 17.18mmol) was added to the mixture to react overnight. The reaction mixture was extracted several times with dichloromethane and saturated saline. The extracted organic phase was used with anhydrous magnesium sulfate. After filtration and evaporation of the solvent, the residue was purified by silica gel column chromatography using dichloromethane/petroleum ether (1:1) as eluent. A buff powder solid product was obtained (2.09g, 84.1%). ^{1}H NMR (500 MHz, Chloroform-d) δ 7.86 (s, 1H), 7.80 (dd, J = 8.0, 3.9 Hz, 3H), 7.76 – 7.66 (m, 4H), 7.42 (tt, J = 6.0, 3.0 Hz, 3H), 2.07 – 1.98 (m, 4H), 0.71 (d, J = 3.9 Hz, 10H).

(5) (7-bromo-9*H*-fluoren-2-yl) (phenyl) methanone (M5)

The synthesis and processing steps for this reaction are the same as for the compound (3). A white powder solid product was obtained (3.78 g, 90.0%). ^{1}H NMR (500 MHz, Chloroform-*d*) δ 8.04 (s, 1H), 7.91 – 7.82 (m, 4H), 7.79 – 7.72 (m, 2H), 7.64 (td, *J* = 7.3, 1.5 Hz, 1H), 7.59 (dd, *J* = 8.2, 1.8 Hz, 1H), 7.54 (t, *J* = 7.8 Hz, 2H).

(6) (7-bromo-9,9-dipropyl-9*H*-fluoren-2-yl) (phenyl) methanone (M6)

The synthesis and processing steps for this reaction are the same as for the compound (4). A buff powder solid product was obtained (2.05g, 82.6%). ^{1}H NMR (500 MHz, Chloroform-*d*) δ 7.89 – 7.83 (m, 3H), 7.81 (dd, *J* = 7.8, 1.6 Hz, 1H), 7.76 (d, *J* = 7.9 Hz, 1H), 7.68 – 7.62 (m, 2H), 7.54 (dd, *J* = 8.8, 7.0 Hz, 4H), 2.06 – 1.95 (m, 4H), 0.74 – 0.68 (m, 10H).

(7) (9,9-dipropyl-9_H_-fluoren-2-yl) (4'-(1-phenyl-1_H_-phenanthro[9,10-_d_] imidazol-2-yl)-[1,1'-biphenyl]-4-yl) methanone (PPIBF)
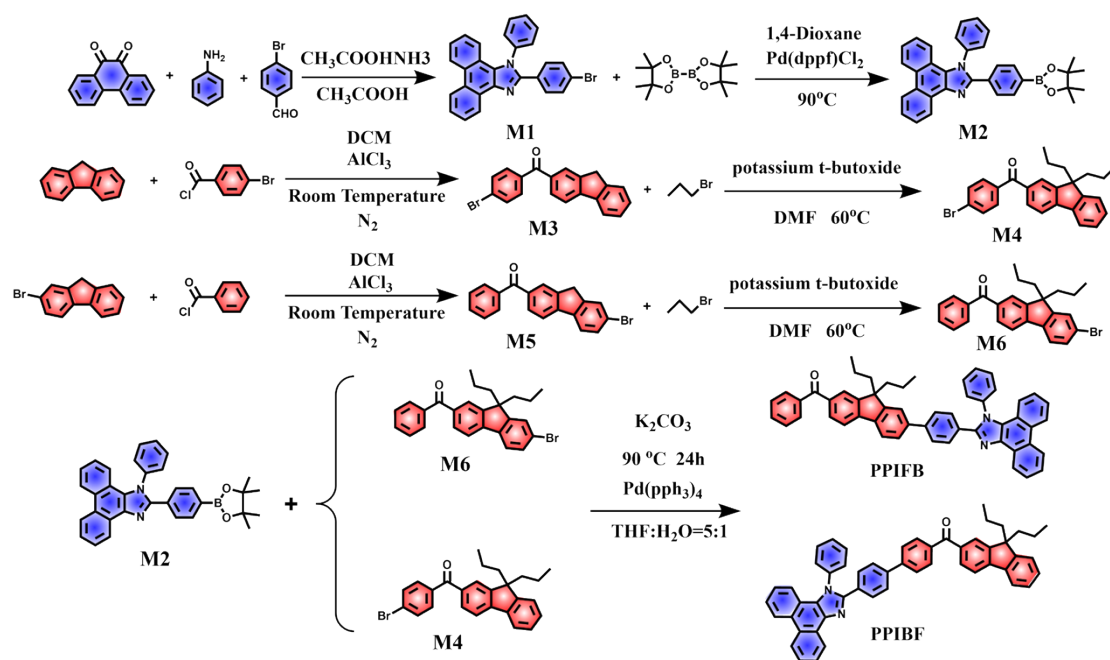
A mixture of (4-bromophenyl)(9,9-dipropyl-9_H_-fluoren-2-yl)methanone (1g, 2.31mmol), 1-phenyl-2-(4-(4,4,5,5-tetramethyl-1,3,2-dioxaborolan-2-yl)phenyl)-1_H_-phenanthro[9,10-_d_]imidazole (1.374g, 2.77mmol), Potassium carbonate (0.48g, 3.47mmol), Tetrakis(triphenylphosphine)palladium (0.11g, 0.10mmol) and Tetrahydrofuran (50ml) were added to the flask and the reaction was refluxed at 110°C for 24h under nitrogen atmosphere. The reaction mixture was extracted several times with dichloromethane and saturated brine. The organic phase obtained from the extraction was dried with anhydrous magnesium sulphate. After filtration and evaporation of the solvent, the residue was purified by silica gel column chromatography using dichloromethane/petroleum ether (3:1) as eluent. A yellow powdery solid product was obtained (1.22 g, 73.2%).^{1}H NMR (600 MHz, Chloroform-d) δ 8.90 (ddd, J = 8.0, 1.5, 0.5 Hz, 1H), 8.80 – 8.76 (m, 1H), 8.74 – 8.68 (m, 1H), 7.91 – 7.87 (m, 3H), 7.81 (dd, J = 7.8, 1.5 Hz, 1H), 7.78 – 7.74 (m, 3H), 7.72 – 7.69 (m, 4H), 7.68 – 7.59 (m, 6H), 7.58 – 7.55 (m, 2H), 7.51 (ddd, J = 8.3, 6.9, 1.3 Hz, 1H), 7.41 – 7.35 (m, 3H), 7.27 (ddd, J = 8.2, 6.9, 1.2 Hz, 1H), 7.19 (dd, J = 8.5, 1.3 Hz, 1H), 1.99 (tdt, J = 13.5, 9.5, 4.3 Hz, 4H), 0.71 – 0.64 (m, 10H). ^{13}C NMR (151 MHz, CDCl$_3$) δ 196.51, 152.04, 150.93, 150.35, 145.71, 144.03, 140.16, 139.91, 138.88, 137.68, 137.36, 136.09, 130.79, 130.42, 130.12, 129.93, 129.46, 129.25, 129.05, 128.47, 128.42, 128.12, 127.46, 127.29, 127.13, 126.89, 126.03, 125.81, 124.87, 124.62, 123.11, 122.92, 121.41, 120.79,

120.57, 119.34, 77.36, 77.14, 76.93, 55.62, 42.61, 17.34, 14.56. HRMS ($C_{53}H_{42}N_2O$): m/z 722.3297 [M+, calcd 722.3293].

(8) phenyl(7-(4-(1-phenyl-1*H*-phenanthro[9,10-*d*] imidazol-2-yl) phenyl)-9,9-dipro-pyl-9*H*-fluoren-2-yl) methanone (PPIFB)

The synthesis and processing steps for this reaction were the same as in (5), and silica gel column chromatography was performed using dichloromethane/petroleum ether (1:1) as eluent. A white powdery solid product was obtained (1.25g, 75.0%). ^{1}H NMR (500 MHz, Chloroform-d) δ 8.94 (d, J = 7.9 Hz, 1H), 8.82 (d, J = 8.4 Hz, 1H), 8.76 (d, J = 8.3 Hz, 1H), 7.91 (s, 1H), 7.89 – 7.77 (m, 6H), 7.76 – 7.60 (m, 13H), 7.55 (t, J = 7.2 Hz, 3H), 7.32 (d, J = 8.1 Hz, 1H), 7.22 (d, J = 8.3 Hz, 1H), 2.05 (d, J = 6.9 Hz, 4H), 0.73 (s, 10H).^{13}C NMR (126 MHz, CDCl$_3$) δ 196.76, 152.73, 151.12, 150.48, 145.06, 141.43, 140.49, 139.47, 138.99, 138.39, 137.63, 136.10, 132.14, 130.27, 130.14, 129.99, 129.88, 129.74, 129.64, 129.37, 129.23, 128.38, 128.35, 128.23, 127.31, 127.28, 126.93, 126.30, 126.28, 125.66, 124.91, 124.58, 124.15, 123.14, 123.09, 122.81, 121.47, 121.00, 120.87, 119.29, 77.27, 77.22, 77.02, 76.76, 55.68, 42.56, 17.32, 14.46. HRMS($C_{53}H_{42}N_2O$): m/z 722.3297 [M+H, calcd 722.3376].

S3 Supplementary Scheme

Scheme S1. Synthetic routes and chemical structures of PPIFB and PPIBF.

S4 Supplementary Figures and Tables
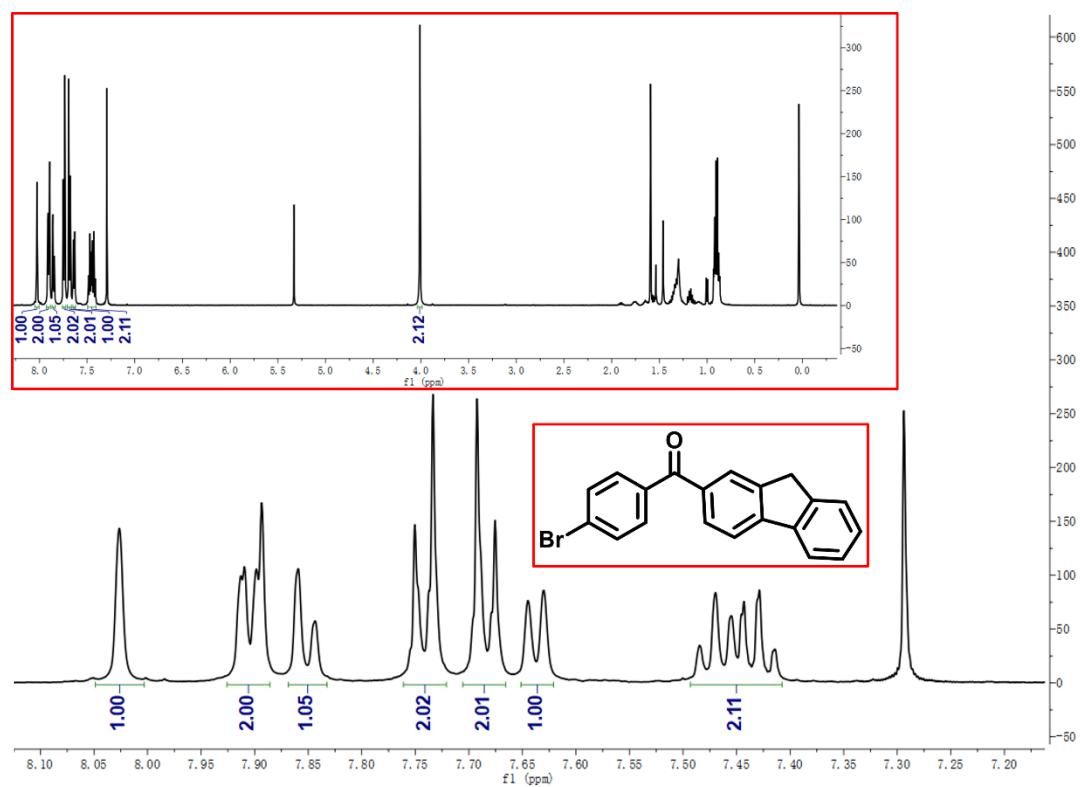
Fig. S1 ¹H-NMR Spectrum of (4-bromophenyl)(9H-fluoren-2-yl)methanone in CDCl₃.
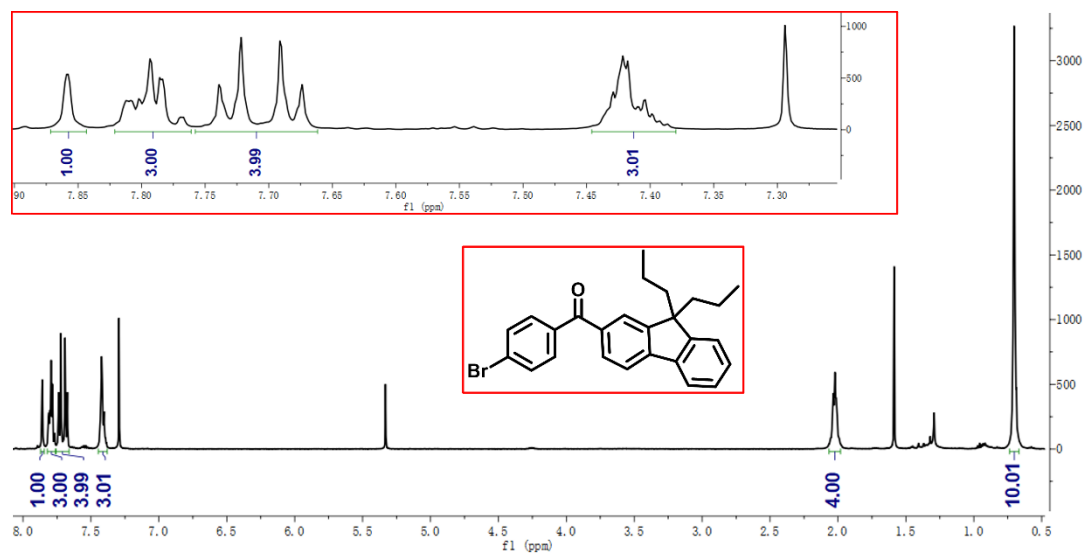
Fig. S2 ¹H-NMR Spectrum of (4-bromophenyl)(9,9-dipropyl-9H-fluoren-2-yl)methanone in CDCl₃.
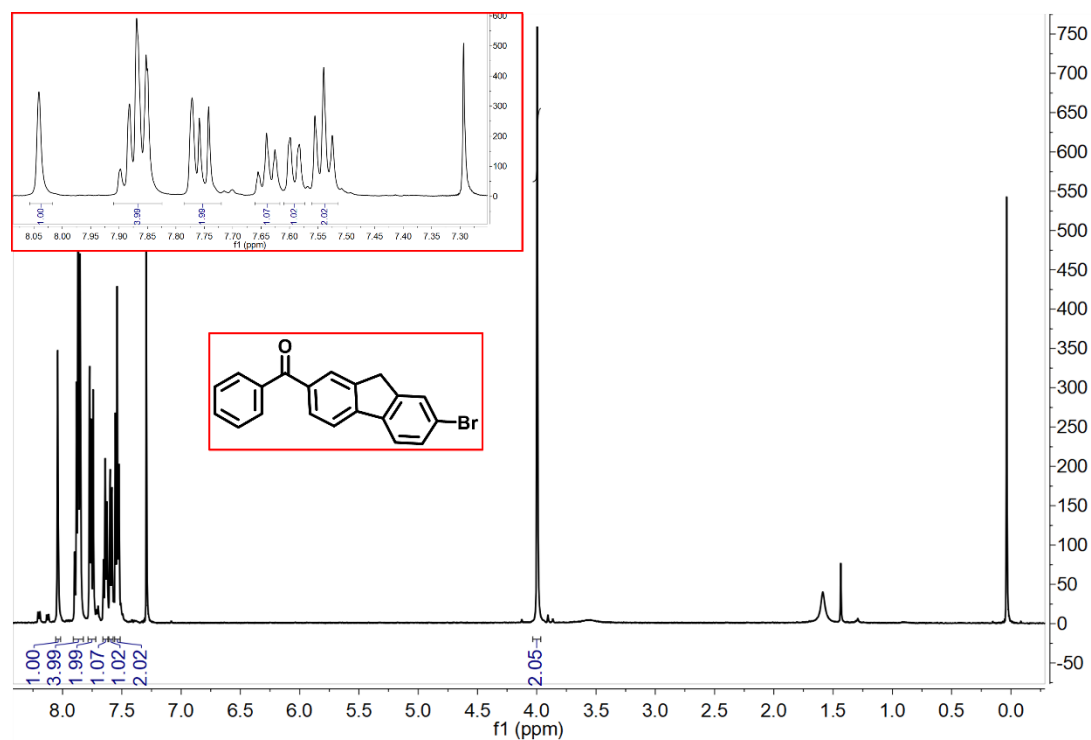
Fig. S3 ^{1}H-NMR Spectrum of (7-bromo-9H-fluoren-2-yl)(phenyl)methanone in
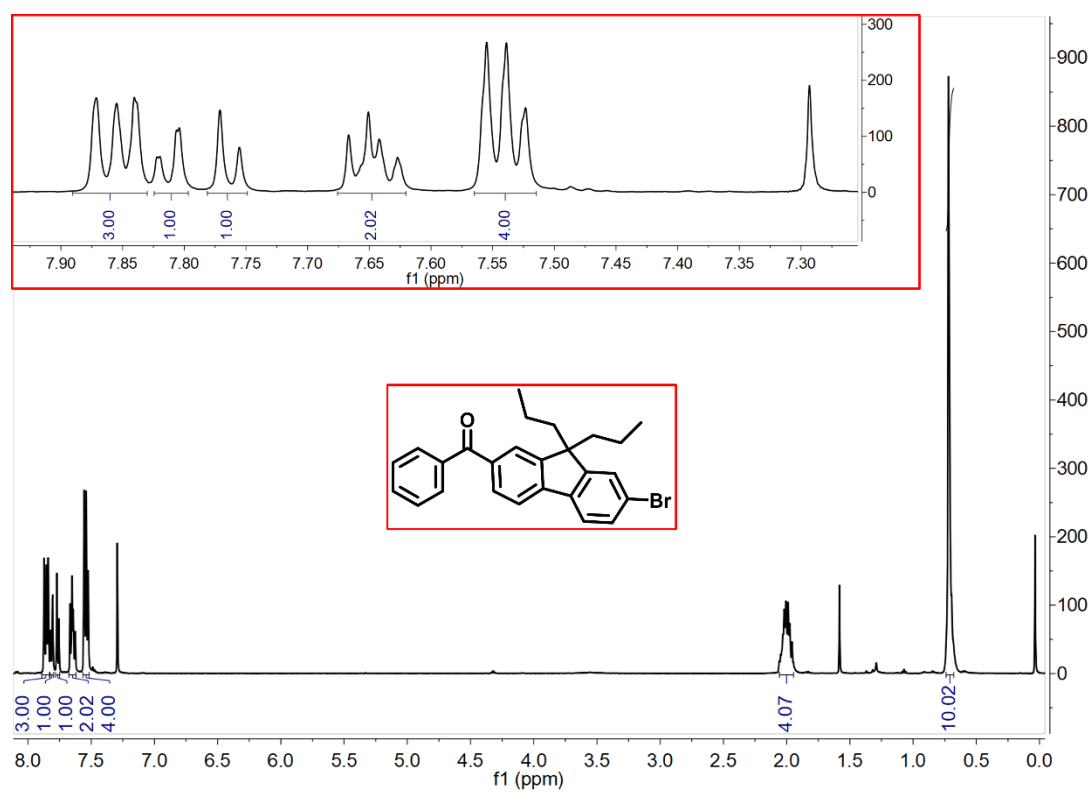
CDCl$_3$.

Fig. S4 ^{1}H-NMR Spectrum of (7-bromo-9,9-dipropyl-9H-fluoren-2-yl)(phenyl)m-

ethanone in CDCl$_3$.
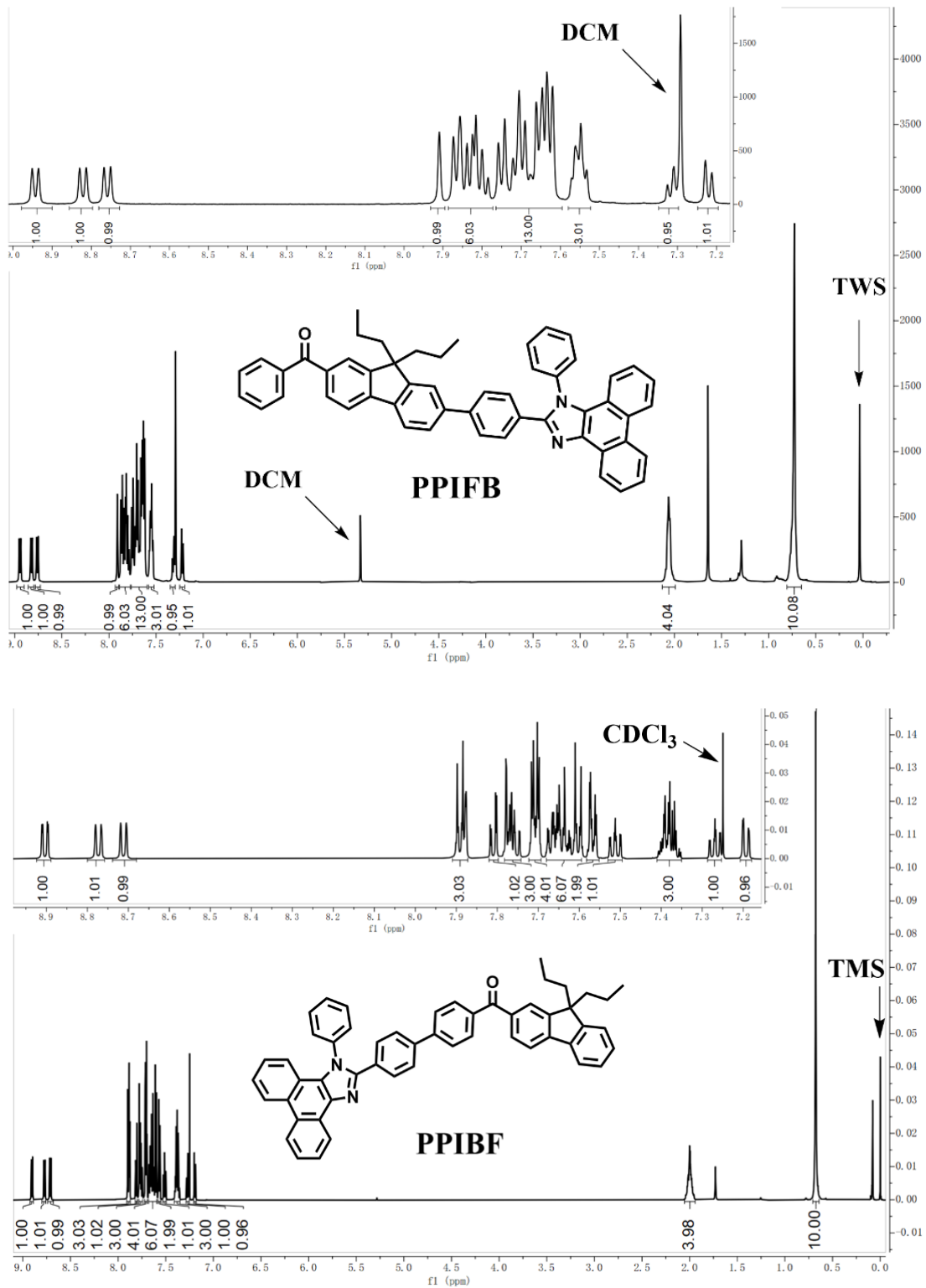
Fig. S5 ^{1}H-NMR Spectrum of PPIFB and PPIBF in CDCl[3].

Fig. S6 ^13^C-NMR Spectrum of PPIFB and PPIBF in CDCl₃.
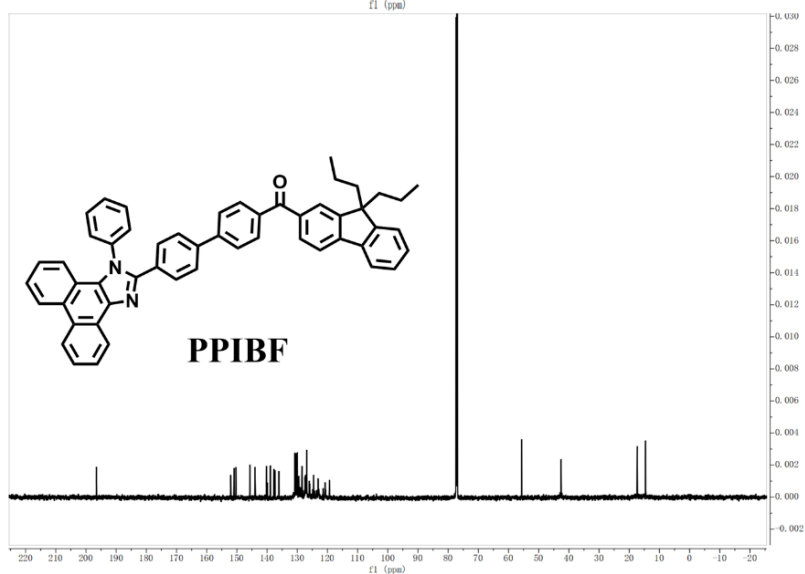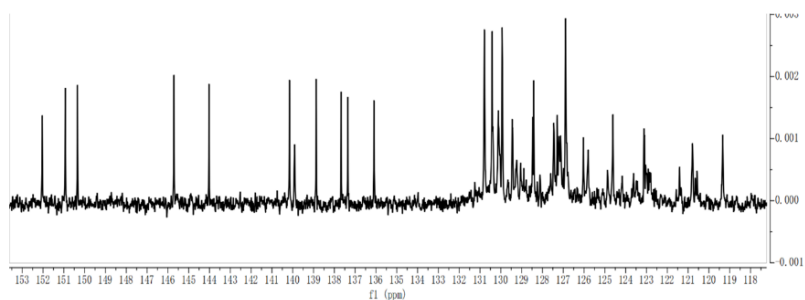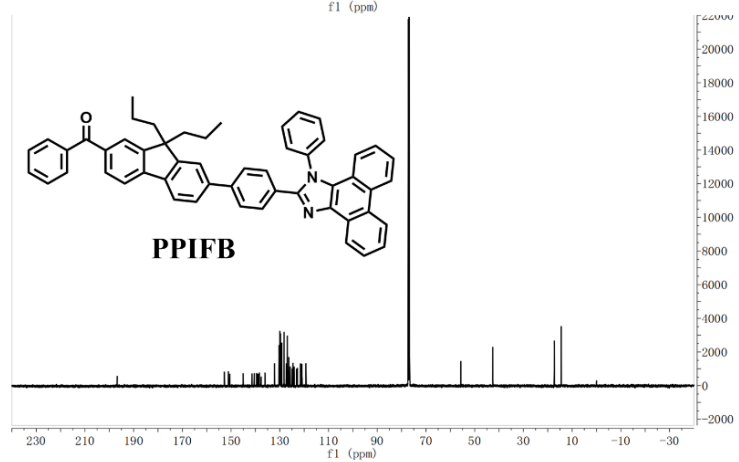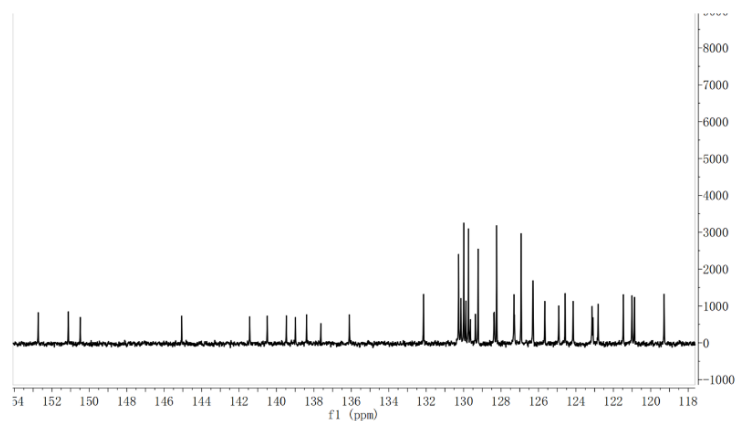
Fig. S6 ^{13}C-NMR Spectrum of PPIFB and PPIBF in CDCl$_3$.
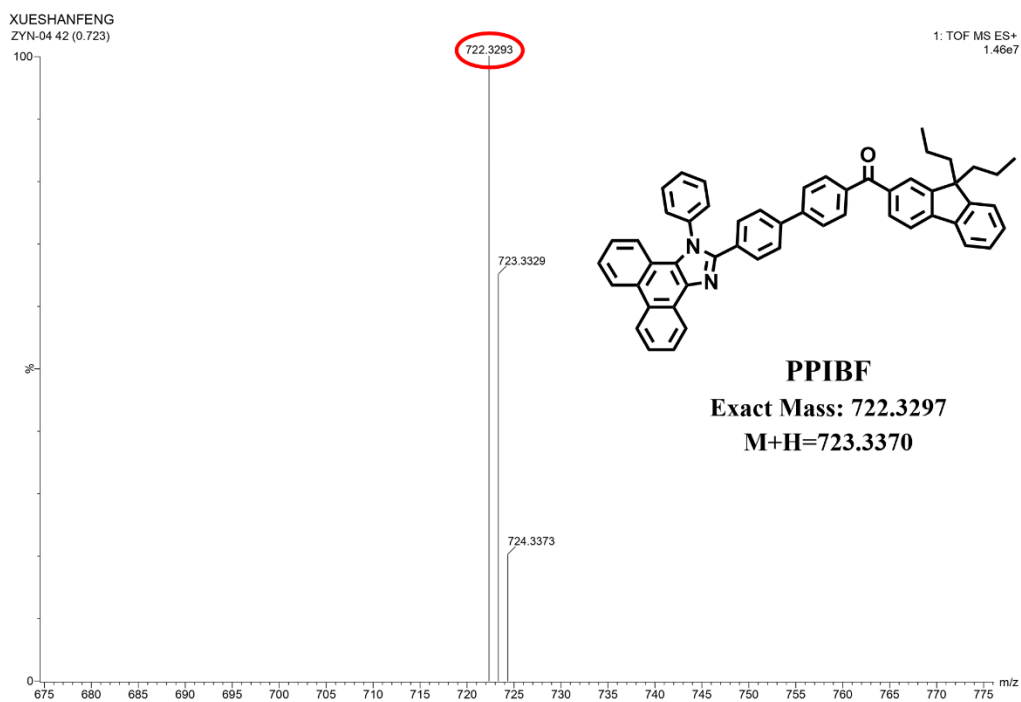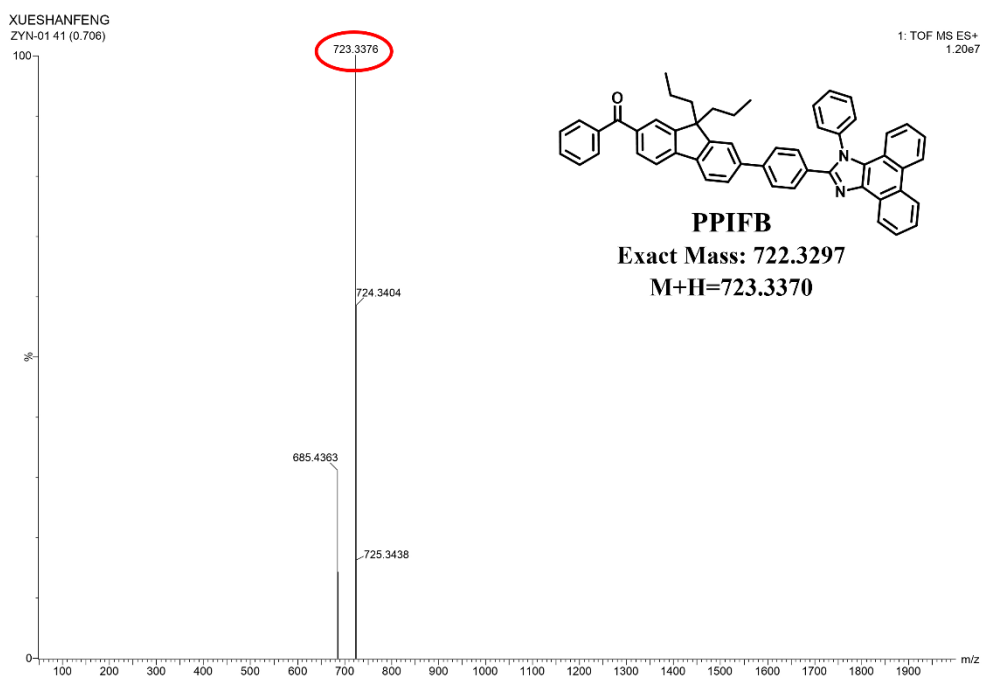
Fig. S7 Mass spectrum of PPIFB and PPIBF.
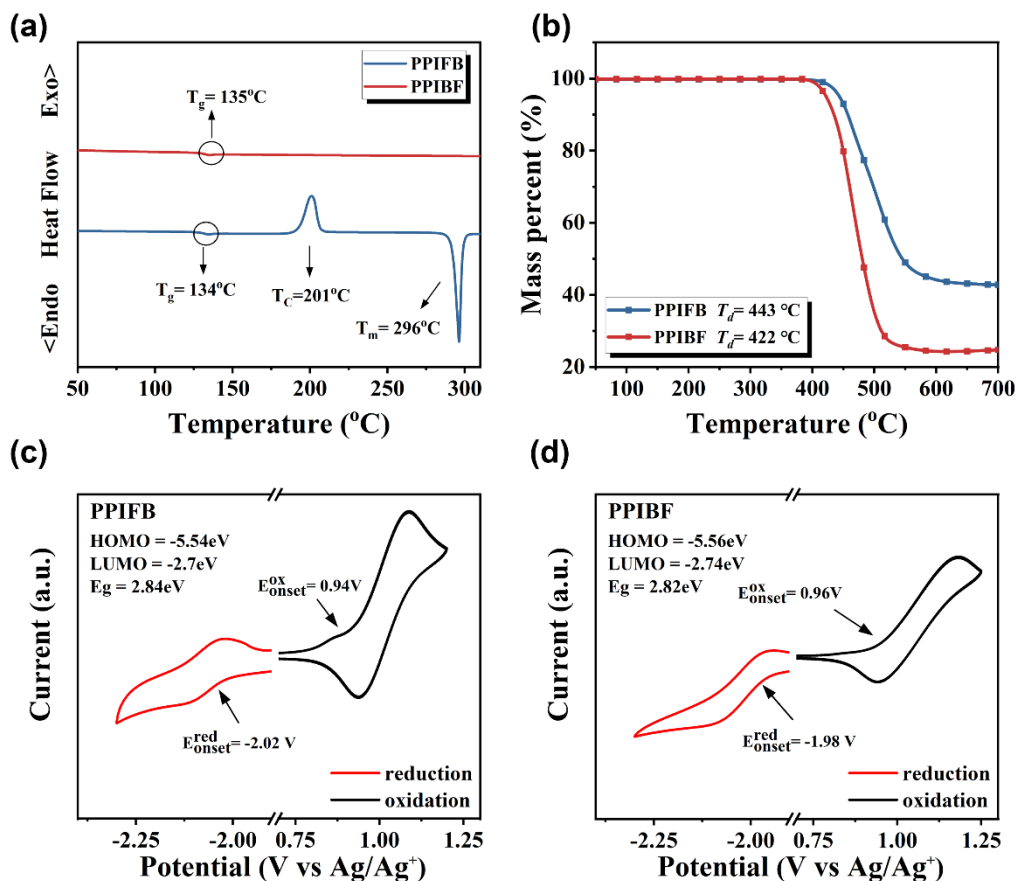
Fig. S8 (a), (b) DSC curves and TGA curves of PPIFB and PPIBF respectively. (c), (d) CV curves of PPIFB and PPIBF.
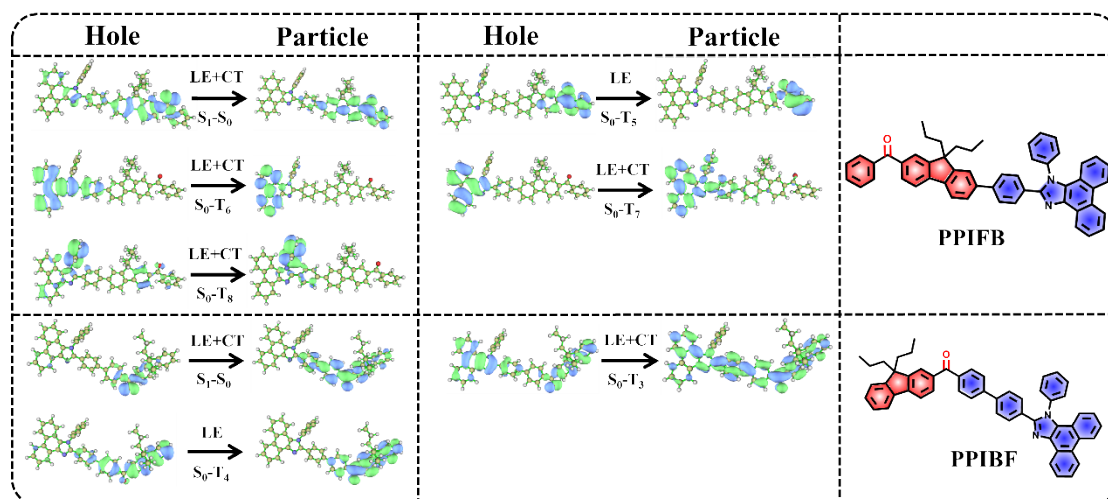

Fig. S9 Potential RISC channels and their natural transition orbitals (NTOs) in PPIFB and PPIBF.
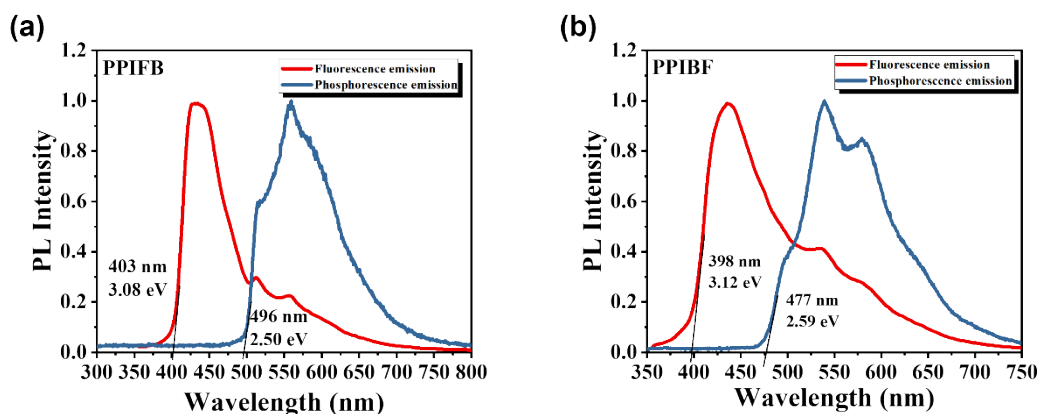
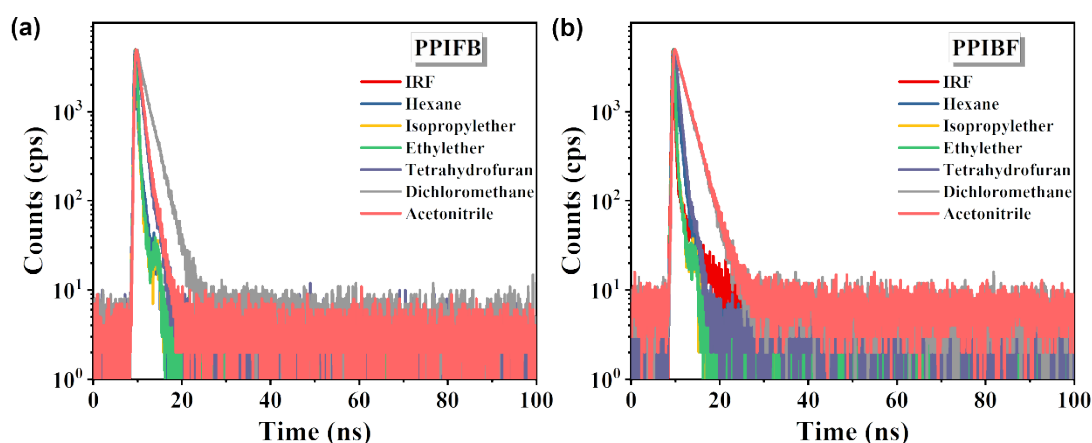**Fig. S10** Fluorescence and phosphorescence spectra of PPIFB and PPIBF in THF (10^{-5} M) at 77K.

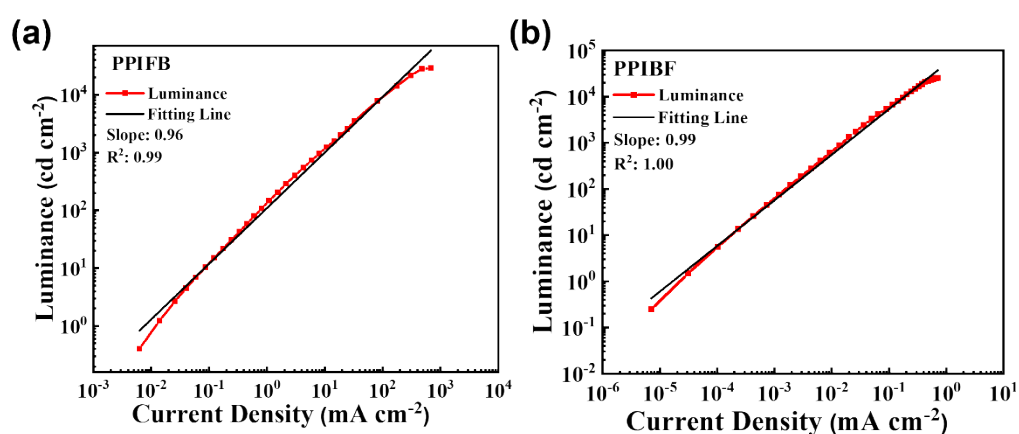**Fig. S11** The lifetimes of PPIFB and PPIBF in solution.

Fig. S12 The current density-luminance curve of non-doped OLED devices.
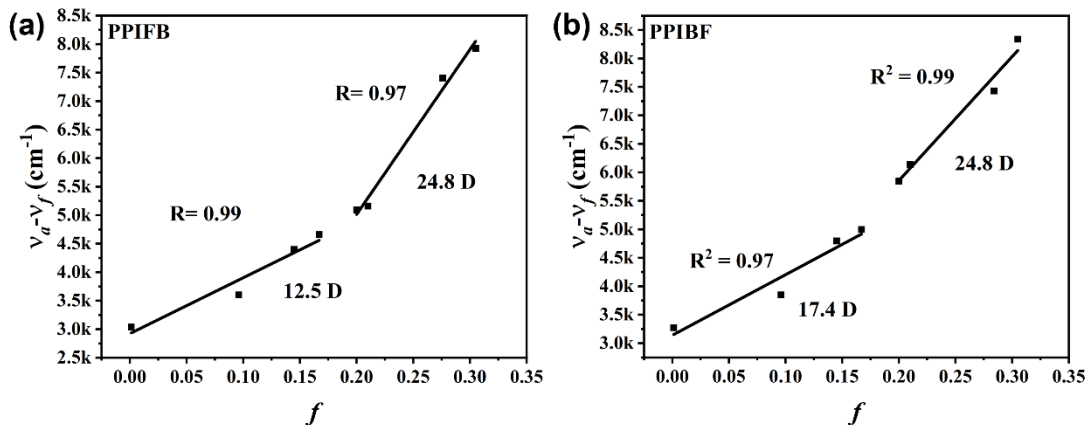
Fig. S13 Linear fitting of the Lippert-Mataga models of PPIFB and PPIBF.
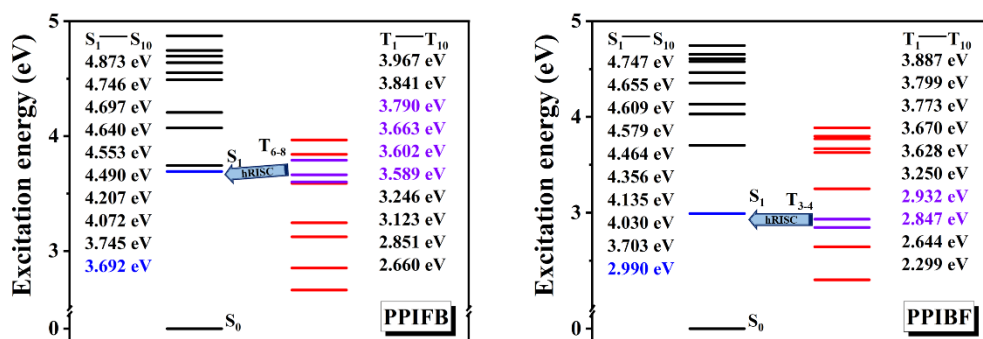

Fig. S14 Energy level diagrams drawn based on NTOs of PPIFB and PPIBF.
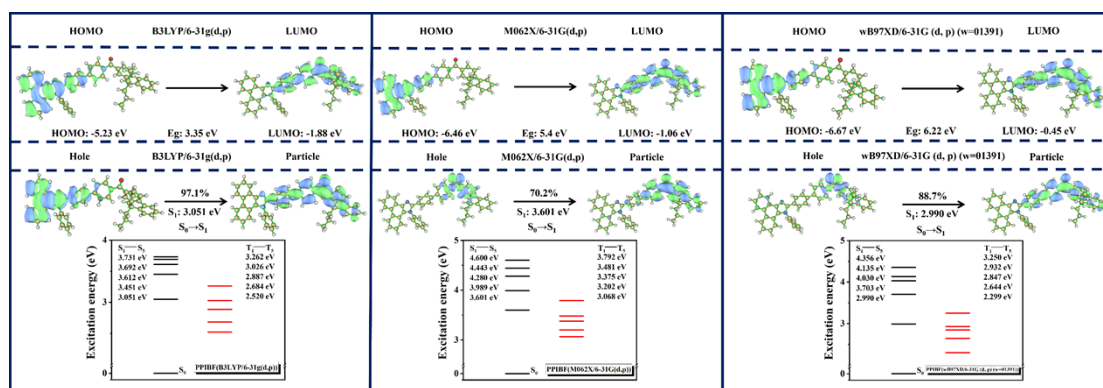

Figure S15. The results of different functional calculations (taking PPIBF as an example).

Table S1. The carrier mobilities of the two luminogens under electric field of 5.0×10^5 V cm^{-1}.

luminogens	Hole mobility [cm^2 V^{-1} s^{-1}]	Electron mobility [cm^2 V^{-1} s^{-1}]
PPIFB	7.65×10^{-7}	1.91×10^{-6}
PPIBF	9.20×10^{-9}	1.10×10^{-6}

Table S2. Crystal data for PPIFB.

Compound	PPIFB
Chemical formula	C53H42N2O
Formula weight	722.89
Crystal system	triclinic
a/Å	8.767(4)
b/ Å	14.833(6)
c/ Å	16.573(6)
α/°	113.305(6)
β/°	102.193(7)
γ/°	90.515(7)
Unit cell volume/ Å3	1924.4(13)
Temperature/K	100(2)
Space group	P -1
Z	2

Density (calculated) /g cm^{-3}	1.248
F(000)	764
Theta range for data collection	2.389 to 27.573
	-10<=h<=8
Index ranges	-17<=k<=17
	-17<=l<=19
Reflections measured	6728
Independent reflections	4415
Rint	0.0603
Completeness to theta = 72.13°	99.1
Max. and min. transmission	0.7677 and 1.000
Data / restraints / parameters	/0/ 507
Goodness-of-fit on F^2	0.949
Final R_1 values ($I > 2\sigma(I)$)	0.0603
Final $wR(F^2)$ values ($I > 2\sigma(I)$)	0.1537
Final R_1 values (all data)	0.0904
Final $wR(F^2)$ values (all data)	0.1660
CCDC number	2324129

References

1 X.H. Lv, L. Xu, W. Cui, Y. Yu, H.Y. Zhou, M. Cang, Q.K. Sun, Y.Y. Pan, Y. Xu, D.H. Hu, S.F.

Xue and W.J. Yang, *ACS Appl. Mater. Interfaces*. 2021, **13**, 970–980.

2 P.N. Murgatroyd, *J. Phys. D: Appl. Phys*. 1970, **3**, 151.